A Large Mammalian Model of Myocardial Regeneration After Myocardial Infarction in Fetal Sheep

Maggie M. Hodges,* Carlos Zgheib, and Kenneth W. Liechty

Laboratory for Fetal and Regenerative Biology, Department of Surgery, University of Colorado Anschutz Medical Campus, Children's Hospital Colorado, Aurora, Colorado, USA.

Maggie M. Hodges, MD, MPH

Submitted for publication November 25, 2018. Accepted in revised form May 14, 2020.

*Correspondence: The Laboratory for Fetal and Regenerative Biology, Department of Surgery, University of Colorado Anschutz Medical Campus, Children's Hospital Colorado, 12631 E. 17th Avenue, C302, Aurora, CO 80045, USA (e-mail: maggie.hodges@cuanschutz.edu).

Objective: Ischemic heart disease accounts for over 20% of all deaths worldwide. As the global population faces a rising burden of chronic diseases, such as hypertension, hyperlipidemia, and diabetes, the prevalence of heart failure due to ischemic heart disease is estimated to increase. We sought to develop a model that may more accurately identify therapeutic targets to mitigate the development of heart failure following myocardial infarction (MI).

Approach: Having utilized fetal large mammalian models of scarless wound healing, we proposed a fetal ovine model of myocardial regeneration after MI.

Results: Use of this model has identified critical pathways in the mammalian response to MI, which are differentially activated in the regenerative, fetal mammalian response to MI when compared to the reparative, scar-forming, adult mammalian response to MI.

Innovation: While the foundation of myocardial regeneration research has been built on zebrafish and rodent models, effective therapies derived from these disease models have been lacking; therefore, we sought to develop a more representative ovine model of myocardial regeneration after MI to improve the identification of therapeutic targets designed to mitigate the development of heart failure following MI.

Conclusions: To develop therapies aimed at mitigating this rising burden of disease, it is critical that the animal models we utilize closely reflect the physiology and pathology we observe in human disease. We encourage use of this ovine large mammalian model to facilitate identification of therapies designed to mitigate the growing burden of heart failure.

Keywords: heart failure, myocardial regeneration, animal models, cardiac fibroblasts

INTRODUCTION

An aging global population and the rising burden of chronic diseases are key to the epidemiologic and demographic transitions observed worldwide.[1] The growing incidence of risk factors for cardiovascular disease, including obesity, diabetes, and hypercholesterolemia, accompanies a growing burden of ischemic heart disease and heart failure.[1,2] Ischemic heart disease is a leading cause of death, and accounts for over $320 billion per year in direct and indirect costs.[3,4] While the incidence of acute myocardial infarction (MI) has decreased, heart failure prevalence increased from 1990 to 2010, with 25% of patients developing heart failure following an MI.[4,5] Access to reperfusion therapy during an MI and evidence-based medical

DOI: 10.1089/wound.2018.0894

management of patients with heart failure have improved over the last 50 years; however, following a heart failure diagnosis, the 5-year mortality remains 54%, highlighting the striking need to develop effective therapies that prevent the development of heart failure following MI.[6]

Following MI, the infarcted myocardium begins the progression through the inflammatory phase of wound healing, which is characterized by production of reactive oxygen species and cytokines that stimulate the synthesis of matrix metalloproteinases (MMPs), degradation of the extracellular matrix (ECM) scaffold, and migration of inflammatory cells into the infarct.[6] During the proliferative phase, inflammatory pathways are downregulated, and cardiomyocytes and epicardial-derived fibroblasts are recruited to the infarct area (IA).[6–8] During the maturation phase, the ECM is remodeled by cross-linking, producing a stiff, collagen-rich scar populated by mature, differentiated fibroblasts.[8,9]

In an effort to understand how to mitigate the progression from MI to the stiffened, fibrotic myocardium found in heart failure, many researchers have turned their attention to understanding how various animal species, such as salamanders and zebrafish, regenerate limbs and tissues following injury. The most widely used models, as well as some of the physiologic characteristics of the studied species are summarized in Table 1. One of the earliest species studied was the zebrafish (*Danio rerio),* which have been noted throughout their lifespan to fully regenerate functional myocardium following apical amputation.[10] In this apical amputation model, zebrafish are noted to regenerate functional myocardium after the fibroblast-rich scar is repopulated by cardiomyocytes thought to be derived from either epicardial progenitor cells or dedifferentiation and proliferation of resident cardiomyocytes.[11,12] However, not only is the amputation model not truly representative of an ischemic event, but also the regenerative capacity of the zebrafish heart is thought to be strongly influenced by the relatively low-pressure system of the two-chamber zebrafish heart, as well as the lifelong presence of mononucleated cardiomyocytes that possess continued proliferative potential.[13] In contrast, the four-chambered adult mammalian hearts are required to generate much higher pressures to maintain forward flow, and adult mammalian cardiomyocytes are binucleated, and therefore lack significant proliferative capacity.[13] These key differences minimize the utility of the zebrafish as a model to study myocardial regeneration after MI with the goal of identifying therapeutic targets to improve outcomes following MI in adult humans.

Discovery of the regenerative potential of early neonatal mice and rats has led to the frequent utilization of rodent models of myocardial regeneration after MI, in which neonatal mice or rats undergo a more representative ligation of the left anterior descending coronary artery, in comparison with the apical amputation model of zebrafish.[14] Unlike the zebrafish model, these neonatal rodent models facilitate evaluation of myocardial regeneration in a four-chambered heart model and have been widely used due to the ease of management of rodent colonies as well as the availability of numerous genetic models that facilitate a deeper understanding of the mechanisms of myocardial regeneration. However, similar to the zebrafish, the cardiomyocytes of neonatal rats and mice are largely mononucleated, thereby retaining their

Table 1. *Animal species modeling myocardial regeneration after myocardial infarction*

Species	*HR (bpm)*	*Blood pressure (SBP/DBP, mmHg)*	*αMHC%*	*Cardiomyocytes (% mononucleate in adulthood)*
Zebrafish	73–152	1.51–2.16	12–53%	95.6%
Danio rerio		0		
Mouse	300–800	110–160	>94–100%	<8.5%
Mus muscularis		80–110		
Rat	250–500	80–180	>94–100%	10–14%
Rattus norvegicus domesticus		55–140		
Sheep	60–120	90–120	0–13%	8%
Ovis aries		100		
Human	60–120	90–140	5–10%	40–75%
Homo sapiens		60–80		

The most widely utilized models of myocardial regeneration after MI are described above, with normal ranges for adult humans included for comparison. Myocardial response to MI has the potential to be strongly influenced by pressure and volume dynamics; therefore, the low-pressure systems of the zebrafish may not be ideal for predicting human physiology.[15,39,40] Similarly, the percent of alpha-myosin heavy chain (αMHC) indicates the proportion of fast-twitch versus slow-twitch muscle fibers that are present in ventricular myocardium.[15,41] Furthermore, the presence of mononucleated cardiomyocytes conveys an inherent regenerative potential that may not be maintained in adult humans; therefore, it is important to consider which species best models human pathophysiology when choosing a model.[15,42,43]

proliferative potential.[15] Furthermore, the size and function of rodent hearts mean the contractile function and myocardial structure of rodent hearts are quite different from that of human hearts, with rodent hearts primarily expressing fast α myosin heavy chain (MHC) (compared to slow β MHC found in human hearts) and only 82% of murine proteases having human orthologs on genome analysis.[13,16,17] These functional and genomic differences also suggest that rodent models of myocardial regeneration after MI may provide limited identification of therapies successful at mitigating the development of heart failure in adult humans.

The limitations of the zebrafish, mouse, and rat models discussed above call into question their utility in developing therapies directed at successfully mitigating the burden of ischemic heart disease in humans. Sheep hearts are known to be similar to human hearts with regard to contractile function, myocardial structure, and both the presence and proportion of binucleate cardiomyocytes throughout the animals' lifespan.[13,15,16] Due to these similarities between the human heart and the sheep heart, we were the first to develop a large mammalian model of myocardial regeneration after MI using fetal sheep.[18] While this model still utilizes the regenerative capacity of the fetus, comparison between the response of the fetal sheep and the adult sheep allows identification of pathways that promote regeneration of functional myocardium in fetal mammals, which may, in turn, promote regeneration of functional myocardium if targeted in adult mammals following MI.

CLINICAL PROBLEM ADDRESSED

Similar to the physiologic response to dermal injury, the heart progresses through inflammatory, proliferative, and remodeling phases following an MI (Fig. 1). The result of this reparative wound healing response is a fibroblast-rich, poorly contractile, fibrotic scar, leading to impaired ventricular function that is a defining feature of heart failure. Numerous animal models exist to study the physiologic response to MI. However, few models exist to study the phenomenon of myocardial regeneration after MI.[10,14] Effective therapies derived from the few, widely used models of myocardial regeneration after MI have been lacking. The source of these translational difficulties may be found in the physiologic differences between large mammals, such as humans, and the study species most commonly utilized—zebrafish and rodents. We now describe a large mammalian model of myocardial regeneration after MI that may enable discovery and testing of therapies

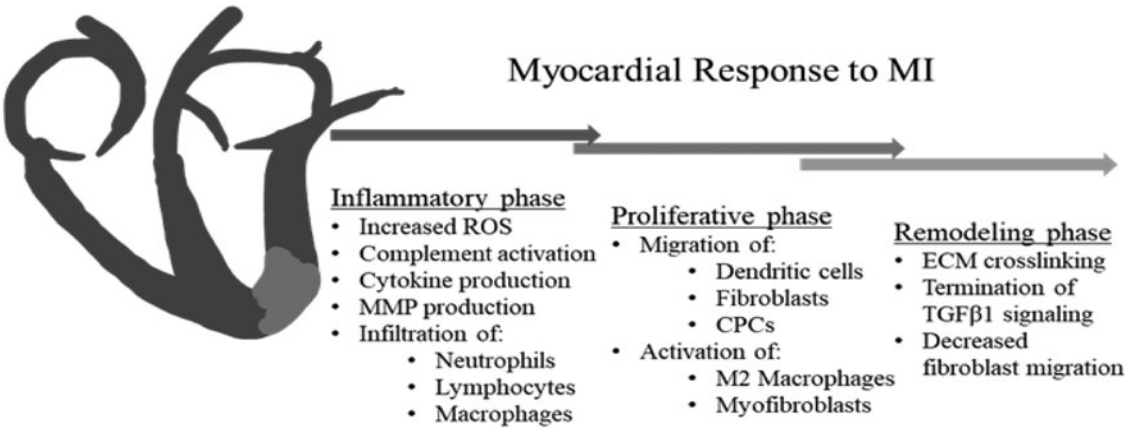

Figure 1. Myocardial response to MI Following myocardial infarction, the heart progresses through overlapping phases of inflammation, proliferation, and remodeling, similar to the response observed in dermal wounds. Cardiomyocyte-derived inflammatory mediators lead to increased production of ROS, release of proinflammatory cytokines, and complement activation. Endothelial activation stimulates additional cytokine and ROS production, as well as infiltration of neutrophils, lymphocytes, mast cells, and macrophages into the IA. MMP production leads to ECM breakdown, with collagen and fibronectin fragments contributing to the continued inflammatory response. During the proliferative phase, the MI, proinflammatory macrophages are thought to transition to a more reparative M2 phenotype, with secretion of anti-inflammatory and profibrotic growth factors decreasing the fibrotic response. Secretion of potent chemokines, such as SDF1α, recruits the migration of CPCs to the IA. Infiltration of dendritic cells that secrete the anti-inflammatory cytokine IL-10 contributes to this M2 macrophage transition. Secretion of profibrotic growth factors such as TGFB1, as well as activation of the renin-angiotensin-aldosterone pathway lead to recruitment of fibroblasts to the infarct area and subsequent activation of fibroblasts to the highly contractile, profibrotic myofibroblast phenotype. The remodeling phase is characterized by continued ECM deposition and crosslinking, with downregulation of TGFB1 signaling, and decreased cellular infiltration as the increased ECM crosslinking inhibits cellular migration. CPC, cardiac progenitor cell; ECM, extracellular matrix; ROS, reactive oxygen species; MMP, matrix metalloproteinase; SDF1α, stromal-derived factor 1 α; TGFB-1, transforming growth factor beta-1; IL-10, interleukin-10; IA, infarct area.

directed at mitigating the development of heart failure following MI.

MATERIALS AND METHODS

Myocardial regeneration after myocardial infarction in fetal sheep

All experiments are approved by The University of Colorado Denver IACUC and performed in compliance with the Guide for the Care and Use of Laboratory Animals (NIH Publication No. 85–23, revised 1996) and the European Convention on Animal Care.

In this model, we utilize fetal Dorset sheep between 65 and 75 days of gestation. We recommend close communication with the sheep breeders during experimental planning, as ewes impregnated during summer months have a high rate of twinning, providing an excellent source of an internal control.

Before surgery, the pregnant ewes are housed socially, provided food and water *ad libitum*, and kept on a standard 12-h diurnal cycle. For 8–12 h before laparotomy, the pregnant ewes are restricted in their PO intake to water alone. Immediately before surgery, the pregnant ewes are placed into holding carts and given an intramuscular (IM) injection of Banamine at 1.1 mg/kg for preoperative pain management. The sheep are then sedated with 11 mg/kg of ketamine and 0.2 mg/kg of diazepam through an intravenous catheter placed in the jugular vein. After sedation, the sheep are then moved to an operating table, where they are endotracheally intubated and anesthetized with 5% isoflurane. Once anesthetized, Cefazolin 1g IV is administered for antibiotic prophylaxis before incision. The sheep are secured in a supine position, using leg straps, and given 600,000 U (2 mls) of penicillin G IM as perioperative prophylaxis. The sheep are mechanically ventilated and monitored throughout the surgery with a pulse oximeter secured to either the ear or nose.

The abdomen of the pregnant ewe is shaved and cleansed with a 70% ethanol solution followed by two coats of Betadine. The field is sterilely draped, and a lower midline laparotomy is performed to expose the gravid uterus. Ultrasound and palpation are used to identify the locations of the fetuses within the uterus. When the fetuses have been identified, a baseline echocardiogram of each fetus is obtained (see further details below). A hysterotomy is performed through which the upper torso of the fetus is partially delivered. A left anterolateral thoracotomy is performed using a 3 cm skin incision over the left 4th–5th intercostal space. The subcutaneous tissues and muscles are divided with electrocautery to insure hemostasis. The heart is best visualized with the use of a miniature Finochietto rib retractor. The pericardium is opened and the heart is externalized. Polypropylene sutures, between 5–0 and 8–0 in size, are used to ligate the distal left anterior descending coronary artery (and any necessary diagonal vessels), to generate a 20–25% apical MI (Fig. 2).

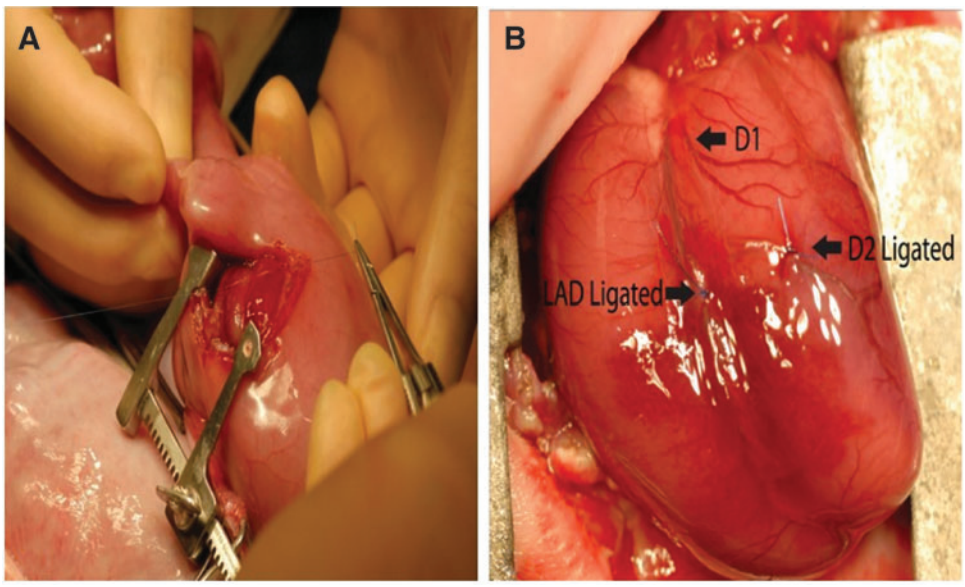

Figure 2. Ovine model of myocardial regeneration after MI The fetal sheep undergoes left anterolateral thoracotomy **(A)**. A miniature Finochietto rib retractor is used to best expose the left ventricle. The LAD is created by ligating the LAD and D2 at a point 40% of the distance between the apex and the base (as shown in **B**), as well as any necessary diagonals, to induce a 20–25% apical infarct. LAD, left anterior descending artery.

Experimental therapies can be administered through direct myocardial administration using a Hamilton syringe (maximum recommended volume 50 μL), or through systemic administration by injection into the umbilical vein (maximum recommended volume 3 mL). Hemostasis is verified and the thoracotomy defect and skin incisions are closed in layers with running 3–0 Vicryl sutures.

The fetus is then returned to the uterine cavity and any amniotic fluid lost during the procedure is replaced using warmed Lactated Ringer's (LR). In addition to LR, the amniotic fluid is treated with 500 mg of ampicillin as prophylaxis against chorioamnionitis. The hysterotomy is closed with two layers of locking 3–0 Vicryl suture, incorporating the amniotic membrane when possible. The fascia of the abdominal wall is closed with running #1 prolene, the deep subcutaneous tissues are reapproximated using interrupted 3–0 Vicryl, and the maternal skin incision is closed with running 4–0 monocryl suture. The pregnant ewe is closely monitored postoperatively until she is freely taking food and water. At this time, she can be returned to social housing, where she will receive 2.2 mg/kg of Banamine through IM injection 24 and 48 h after the surgery for postoperative analgesia.

Before euthanasia, the pregnant ewe is again sedated, endotracheally intubated, and mechanically ventilated, with anesthesia maintained using isoflurane. The prior laparotomy and hysterotomy incisions are reopened and the fetuses are identified by palpation and ultrasound. Quantitative echocardiography is performed, to quantify both infarct length and ejection fraction (EF, %) following MI. The pregnant ewes are then euthanized through IV administration of sodium pentobarbital (1 mL/10 lbs body weight). Once euthanized, the hysterotomy is reopened, the fetus is externalized, and euthanasia of the fetus is ensured by injection of 1 mL of sodium pentobarbital into the umbilical vein. When cardiac activity has ceased, the fetal hearts are collected and processed.

MI in adult sheep

Immediately before surgery, the adult sheep are placed into holding carts and given an IM injection of Banamine at 1.1 mg/kg for preoperative pain management. The sheep are then sedated with 11 mg/kg of ketamine and 0.2 mg/kg of diazepam through an intravenous catheter placed in the jugular vein. After sedation, the sheep are then moved to an operating table, where they are endotracheally intubated and anesthetized with 5% isoflurane. Once anesthetized, cefazolin 1g IV is administered before incision and for antibiotic prophylaxis. The sheep are secured supine, with a slight bump under the left chest, to provide a slight right lateral decubitus position. The sheep are mechanically ventilated and monitored throughout the surgery with a pulse oximeter secured to either the ear or nose. Two-dimensional transthoracic echocardiography was performed to determine the preoperative ejection fracture (EF) of individual sheep. The left chest wall is then shaved and cleansed with a 70% ethanol solution followed by two coats of Betadine. A left anterolateral thoracotomy is performed along the left, 3rd intercostal space, and a self-retaining, Finochietto retractor is used to open the surgical field and reveal the left anterior descending artery (LAD). Polypropylene sutures, between 3–0 and 8–0 in size, are used to ligate the distal left anterior descending coronary artery (and any necessary diagonal vessels), to generate a 20–25% apical MI. Successful ligation is indicated by pallor of the left ventricular myocardium after ligation of the LAD. Similar to the fetal model, experimental therapies can be administered through direct myocardial administration using a Hamilton syringe or through systemic administration by injection into the internal jugular vein. Hemostasis is verified and the thoracotomy defect and skin incisions are closed in layers with running 0 Vicryl sutures.

The sheep are closely monitored postoperatively until they are freely taking food and water. At this time, the sheep can be returned to social housing, where they will receive 2.2 mg/kg of Banamine through IM injection 24 and 48 h after the surgery for postoperative analgesia.

Before euthanasia, the sheep is again sedated, endotracheally intubated, and mechanically ventilated, with anesthesia maintained using isoflurane. Quantitative echocardiography is performed, to quantify both infarct length and EF, % following MI. The sheep are then euthanized through IV administration of sodium pentobarbital (1 mL/10 lbs body weight). Once euthanized, the chest is opened by median sternotomy, and the heart is collected *en bloc* for further processing.

Echocardiographic measurements

Two-dimensional echocardiography is performed in all sheep before MI (baseline), immediately after MI, and before euthanasia. Left ventricular function is calculated using the modified Simpson method by approximating left ventricular end systolic volume (LV ESV) and left ventricular end di-

astolic volume (LV EDV) through ventricular endocardial area tracings in the apical 4-chamber and 2-chamber view and calculating the left ventricular ejection fraction (LVEF) by dividing the difference in LV ESV and LV EDV by LV EDV [LVEF(%) = (LV ESV–LV EDV)/LV EDV × 100].[19] Infarct size was estimated as the ratio of infarct length to LV long-axis length in diastole.[18]

Sample preparation

Meticulous processing of the hearts, both for sample preparation as well as for tissue culture, cannot be understated, as the heart is a heterogenous organ, with significant differences in the behavior and response of tissues when comparing atria to ventricles, left to right, apex to base, and endocardial to myocardial.[13]

Following *en bloc* removal of the hearts, the atria are removed, and the right ventricle is removed, leaving the conical left ventricle (LV) for further processing. The LV is divided into three longitudinal slices, with each slice incorporating IA, borderzone (BZ), and remote zone (RZ). One of these slices is frozen in optimal cutting temperature compound for histologic evaluation, and the remaining two slices are further subsectioned into IA, BZ, and RZ, with the subsections flash frozen in liquid nitrogen to process for RNA and protein analysis (Fig. 3).

Histology

Heart subsections are subsequently fixed in 4% paraformaldehyde for a minimum of 72 h and then processed using a Leica 1050 histoprocessor (Leica Microsystems, Buffalo Grove, IL). Four micrometers of paraffin sections is mounted on Fisher Plus slides (Fisher Scientific, Pittsburgh, PA), before being incubated at 52°C overnight, and deparaffinized in xylenes for 10 min (×3), followed by rehydration in graded ethanol (2×100%, 2×95%, and 2×75%) to distilled water. We use either hematoxylin and eosin or Masson trichrome staining, as previously described, to evaluate gross architecture of the myocardium and collagen staining of the infarct.[18]

In vitro models

To obtain cardiac fibroblasts for *in vitro* experiments, uninfarcted hearts are obtained. The hearts are washed in 70% ethanol for 60 s before being washed three times in ice-cold phosphate-buffered saline (PBS) to remove blood and extraneous tissue. The atria and valves are removed, and the LV is separated from the right ventricle and septum before the pericardium is removed by sharp dissection. The hearts are washed in room-temperature PBS before being incubated for 18 h in PBS with 10 mM HEPES, 0.25% trypsin (USB 22705), and 0.54 mM EDTA (pH 7.4) at 4°C. Hearts are then incubated in PBS with 10% horse serum, 5% fetal bovine serum (FBS), 10 mM HEPES buffer, and 1% penicillin/streptomycin for 30–60 min at 37°C before being repeatedly pipetted against the base of a tissue culture dish using a 5 mL transfer pipette until the tissue is completely dissociated. The resulting cell suspension is subsequently centrifuged at 35 *g* at 4°C for 5 min, the supernatant is removed, and the cells are washed with PBS containing 10% horse serum, 5% FBS, and 1% penicillin/streptomycin before being resuspended in DMEM with 10% horse serum, 5% FBS, and 1% penicillin/streptomycin. This cell solution is filtered through a 70 μm mesh cell strainer on to 12-well dishes before being incubated at 37°C in 5% CO_2. The presence of beating cardiomyocytes was noted after 24 h of culture; however, these beating cells were no longer present following one passage with 0.25% trypsin-EDTA. Cardiac fibro-

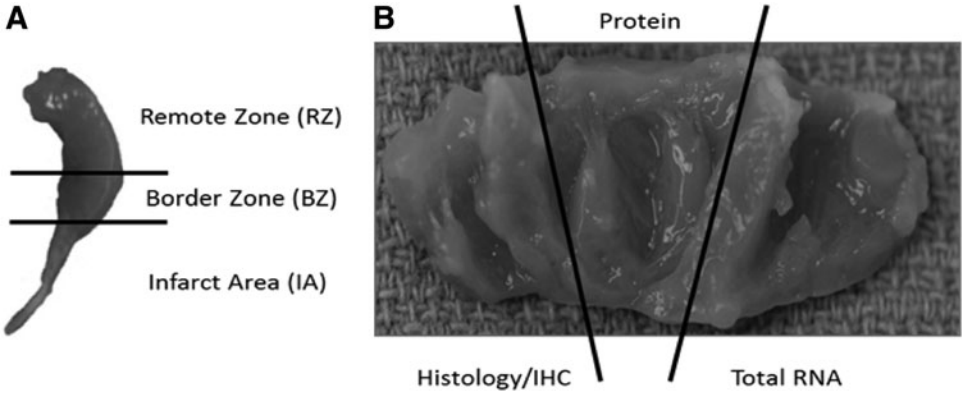

Figure 3. Subsectioning of heart samples The left ventricle is sectioned into three areas **(A)** RZ, BZ, and IA. Each of these areas is then divided into three parts **(B)** for protein, gene, and histological analysis. RZ, remote zone; BZ, border zone.

blast identity is confirmed by evaluation of cell morphology and vimentin staining, although DDR2 positivity has also been suggested as a strong marker of cardiac fibroblast identity.[7]

Ovine specific microarray

The ovine hearts are subsectioned as described above. To extract total RNA for microarray analysis, subsections of IA and RZ from both adult and fetal hearts, both 3 and 30 days after MI ($n=4$ in each group), are homogenized in TRIzol (Invitrogen and Life Technologies, Carlsbad, CA). The High-Capacity cDNA Reverse Transcription Kit (Applied Biosystems, Foster City, CA) is used to reverse transcribe complementary DNA (cDNA) from total RNA. cDNA is labeled with fluorescent dCTP and mixed probes are hybridized to the oligonucleotide ovine-specific microarrays (Agilent Technologies, Foster City, CA). Using the Gene Ontology Consortium database, mammalian genes identified as belonging to the gene groups "response to wounding" (GO: 0009611), "inflammatory response" (GO: 0006954), "cell cycle" (GO:0007049), "cell migration" (GO: 0016477), "cell proliferation" (GO: 0008283), "apoptosis" (GO: 0006915), and "extracellular matrix" (GO: 0031012). Gene expression in the IA is compared to gene expression in the RZ to identify genes altered by MI, and gene expression is considered significantly altered if a p-value of less than 0.05 is obtained after using the Statistical Analysis of Microarray method to compare the gene expression in the IA and the RZ.[20,21]

Quantitative polymerase chain reaction

We evaluate mRNA, microRNA, and long noncoding RNA in our models; therefore, we advise the extraction of total RNA from these limited tissue samples. For evaluation of mRNA, total RNA is extracted and purified after samples are homogenized in TRIzol (Invitrogen, Life Technologies). cDNA is constructed from RNA using the SuperScript First-Strand Synthesis System (Invitrogen, Life Technologies). Random primers are used for reverse transcription, and real-time quantitative polymerase chain reaction (PCR) is performed using the ABI 7900 real-time PCR thermal cycler (Applied Biosystems). Samples are amplified in triplicate using ovine-specific primers for the genes of interest. Relative gene expression is compared using the $\Delta\Delta$Ct method.[22]

RESULTS

Comparing the results from the fetal MI model to the adult MI model, we have observed marked differences between the fetal and adult response to MI with regard to functional outcome, ECM deposition, inflammatory profiles, and cellular response. When comparing the EF of adult and fetal sheep, 3 and 30 days after MI, adult sheep were noted to have a decreased EF 3 days post-MI and a significant worsening of their EF 30 days following MI, as seen in Fig. 4B. In contrast, fetal sheep demonstrated preserved EF both 3 and 30 days post-MI. Similarly, infarct length was noted to increase by14.5% in adult sheep 30 days following MI, while infarct length was unmeasurable in fetal sheep 30 days following MI, as no wall motion abnormality could be detected (Fig. 4C).[18]

The functional impairments observed in the adult hearts 30 days following MI correspond to grossly visible ventricular fibrosis and ventricular wall thinning, while the fetal hearts demonstrated no gross evidence of scar formation 30 days after MI (Fig. 5A, B). Histologically, the adult hearts demonstrate apical myocyte loss and replacement of the infarct with a collagen-rich scar, while fetal hearts demonstrate restoration of functional myocardium with scant interstitial collagen deposition observed at the site of the infarct (Fig. 5C–F). Furthermore, we have reported that analysis of ovine-specific microarray data demonstrated significant upregulation of genes related to ECM remodeling in adult hearts both 3 and 30 days after MI, when compared to fetal hearts at the same time points, as seen in Fig. 5G.[23] More recently, we have demonstrated that the decreased collagen deposition and ECM-related gene expression that characterize the fetal response to MI are associated with differential expression of the profibrotic growth factor transforming growth factor beta-1 (*TGFB1*), while adult hearts demonstrate marked upregulation of *TGFB1* both 3 and 30 days after MI; fetal hearts lack *TGFB1* upregulation at either time point.[24]

The increased fibrosis and decreased function of the adult heart following MI are associated with an increased inflammatory response when compared to the regenerative, fetal response to MI.[18,23] Adult infarcts demonstrated a robust infiltration of $CD45^+$ inflammatory cells post-MI, with continued inflammation and apoptosis observed 30 days following MI (Fig. 6A–F). In contrast, fetal infarcts had a markedly attenuated inflammatory cellular response in comparison to the adult response, with near complete resolution of the inflammatory infiltrate 30 days post-MI and no evidence of apoptosis 30 days post-MI. These cellular changes are accompanied by significantly reduced expression of the proinflammatory cytokines *IL-6* and *IL-8* in

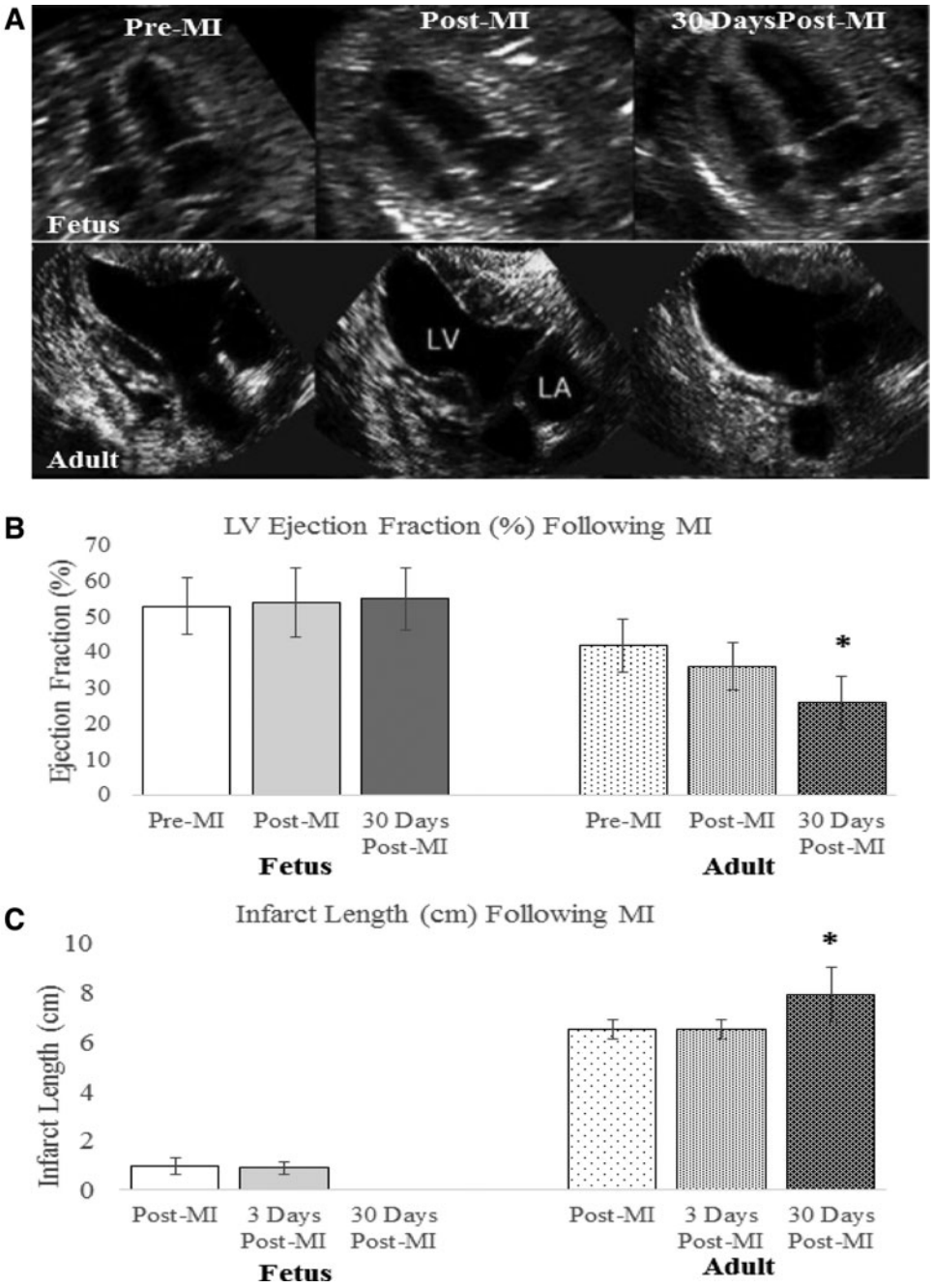

Figure 4. Functional restoration after MI in fetal sheep **(A)** Cardiac function declines in the adult hearts following MI, whereas the fetal hearts show restoration of function. Serial end-systolic echocardiographic views show no evidence of LV dilation or infarcted myocardium at 30 days in the fetus, whereas the adult hearts show dilation of the LV, 30 days following infarction with a large anteroapical infarct. **(B)** EF measured by quantitative echocardiography is unchanged in the fetus at 3 days ($p=0.37$) and 30 days ($p=0.31$) following infarction. In the adult, the EF has significantly declined by 30 days following MI (*$p<0.05$ vs. adult pre-MI and post-MI). **(C)** Absolute infarct length defined as the length of akinetic myocardium measured by echocardiography is unchanged at 3 days following infarction ($p=0.72$), but decreases to zero in the fetus at 30 days following infarction (*$p<0.05$ vs. fetal post-MI). In the adult, the absolute infarct length is also unchanged at 3 days following infarction ($p=1.00$), but increases over a period of 30 days following infarction (*$p<0.05$ vs. adult post-MI). EF, ejection fraction; LV, left ventricular.

the fetal infarcts compared to the adult infarcts, both 3 and 30 days post-MI (Fig. 6H). Looking more broadly, ovine-specific microarray also demonstrated marked reduction in the expression of inflammation-related genes in the fetal infarcts 3 and 30 days post-MI, when compared to the expression of inflammation-related genes in the adult infarcts (Fig. 6G).

The regeneration of functional myocardium observed in fetal hearts is also accompanied by striking differences in the cellular response when compared to the established cellular response

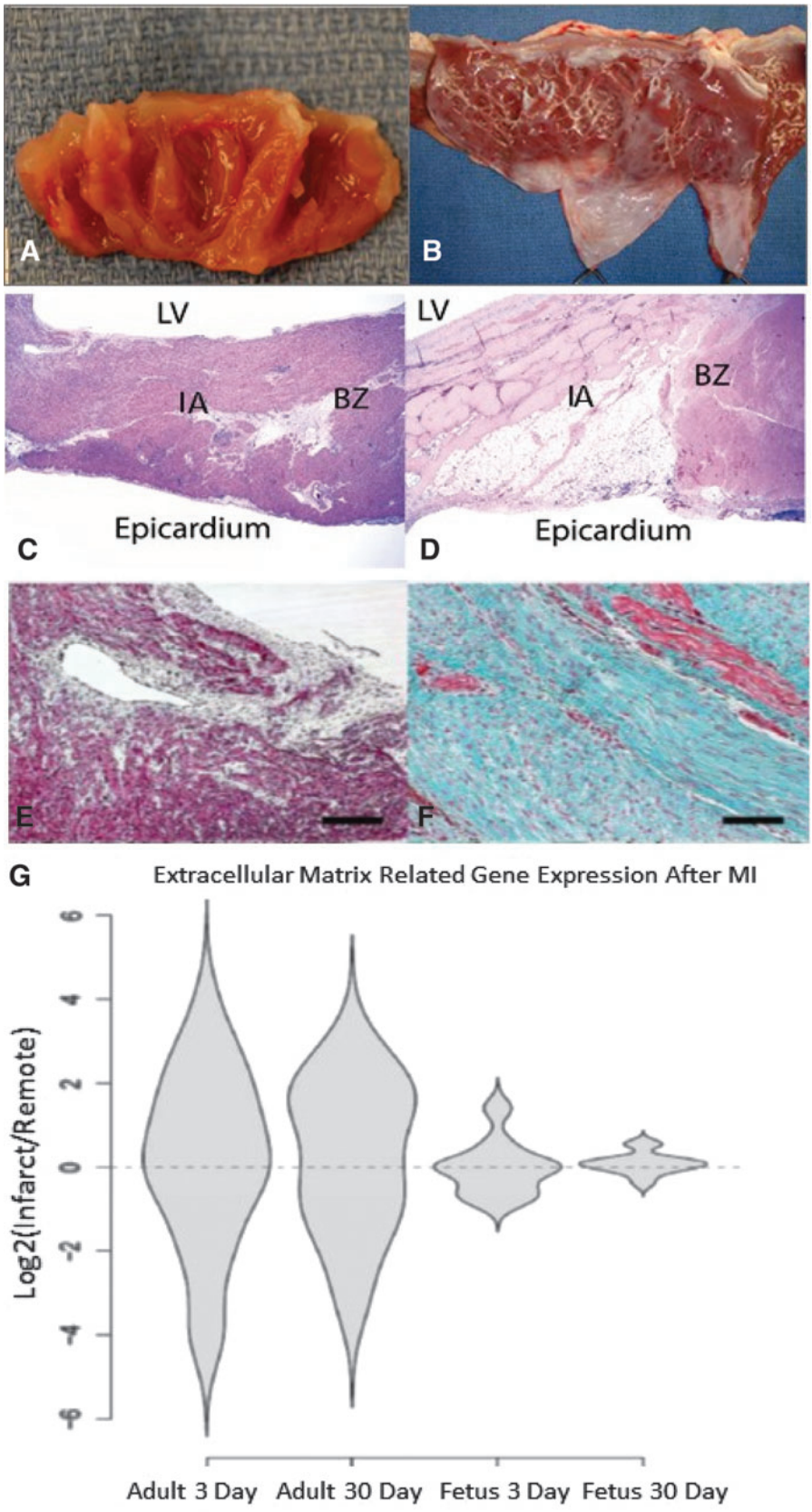

Figure 5. Differential regulation of ECM after MI **(A–F)** Fetal hearts regenerate without scar formation following MI. Four weeks after myocardial infarction, **(A)** fetal hearts show no gross evidence of fibrosis, while **(B)** adult hearts show apical fibrosis and ventricular wall thinning. H&E staining at 4 weeks demonstrates **(C)** no evidence of myocyte loss or ventricular wall thinning in the fetal heart (I) infarct or BZ and **(D)** significant myocyte loss and ventricular wall thinning in the adult infarct (I) (20×). Masson's trichrome staining at 4 weeks following MI confirms that there is **(E)** minimal fibrosis in the fetal infarct (100×) and **(F)** an exuberant fibrotic response in the adult infarct (100×). **(G)** Adult infarcts demonstrated a persistent increase in the expression of "extracellular matrix" genes from day 3 to day 30, whereas the fetal infarct gene expression returned to baseline by 30 days. *Violin plots* for the genes related to the gene ontology term ECM. The y-axis represents the $\log_2$ of the ratio of the infarct to remote region average gene expression. The *violin shapes* represent the distribution of the $\log_2$ ratios in each group. (20 genes; $p < 0.005$, Student's *t* test).

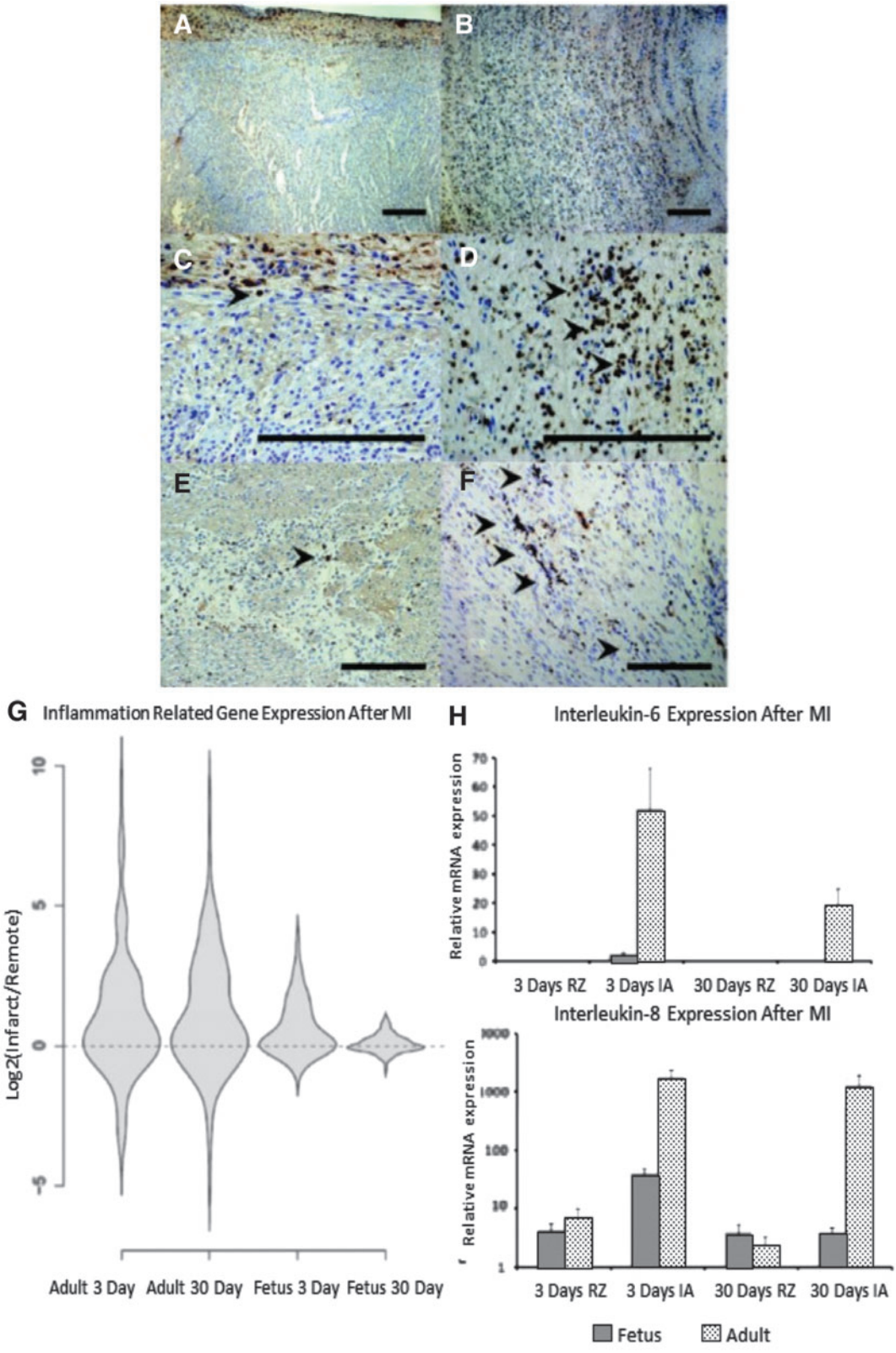

Figure 6. Differential inflammatory response after MI **(A–F)** Decreased infiltration of inflammatory cells following myocardial infarction in fetal verses adult hearts. Seven days following infarction, CD45 immunohistochemistry demonstrated that the fetal heart **(A-100×, C-400×)** shows minimal numbers of inflammatory cells, while the adult heart **(B**-100×, **D**-400×**)** shows a large infiltrate, with CD45 positive cells marked by *arrowheads*. At 4 weeks following infarction, the number of inflammatory cells in both the **(E)** fetal and **(F)** adult hearts has decreased, but the adult heart has persistent scattered areas of inflammation not seen in the fetus (200×). **(G)** Adult infarcts demonstrated a persistent increase in the expression of "inflammatory response" genes from day 3 to day 30, whereas the fetal infarct gene expression returned to baseline by 30 days. *Violin plots* for the genes related to the GO term "inflammatory response." The *y*-axis represents the log2 of the ratio of the infarct to remote region average gene expression. The *violin shapes* represent the distribution of the log2 ratios in each group. (162 genes; $p < 0.005$, Student's *t* test). **(H)** High expression of proinflammatory cytokines *IL-6* and *IL-8* in adult infarcts versus fetal infarcts. Real-time PCR analysis of mRNA for *IL-6* and *IL-8* in fetal and adult hearts at 3 and 30 days after MI. Both *IL-6* and *IL-8* are highly expressed in the adult infarct 3 and 30 days after MI. However, in the fetus, 3 days after MI, *IL-6* gene expression is slightly increased and completely disappears after 30 days.

observed in adult hearts. Staining of the fetal infarcts with BrdU revealed that the response of the fetus to MI is followed by robust cardiomyocyte proliferation consistent with myocardial regeneration (Fig. 7A), in contrast to established literature describing the lack of cardiomyocyte proliferation in the adult response to MI.[18,25] The regeneration of functional myocardium in fetal sheep is also associated with restoration of microvasculature in the IA, with increased levels of vascular endothelial growth factor (*VEGF*); in contrast, adult infarcts remain fibrotic, poorly vascularized, and without significant increase in *VEGF* in the IA, as shown in Fig. 7B.[26] By treating fetal infarcts with a lentiviral construct designed to replace functioning *SDF1α* with a nonfunctional mutant *SDF1α* transgene, we were able to inhibit cardiac progenitor cell (CPC) recruitment to the IA, as shown in Fig. 8A.[27] Using this method, inhibition of CPC recruitment to the IA successfully impaired myocardial regeneration in the fetal model, suggesting that the lack of CPC recruitment observed in adult mammals may be the reason adult mammalian hearts do not regenerate following MI.[27,28] In ad-

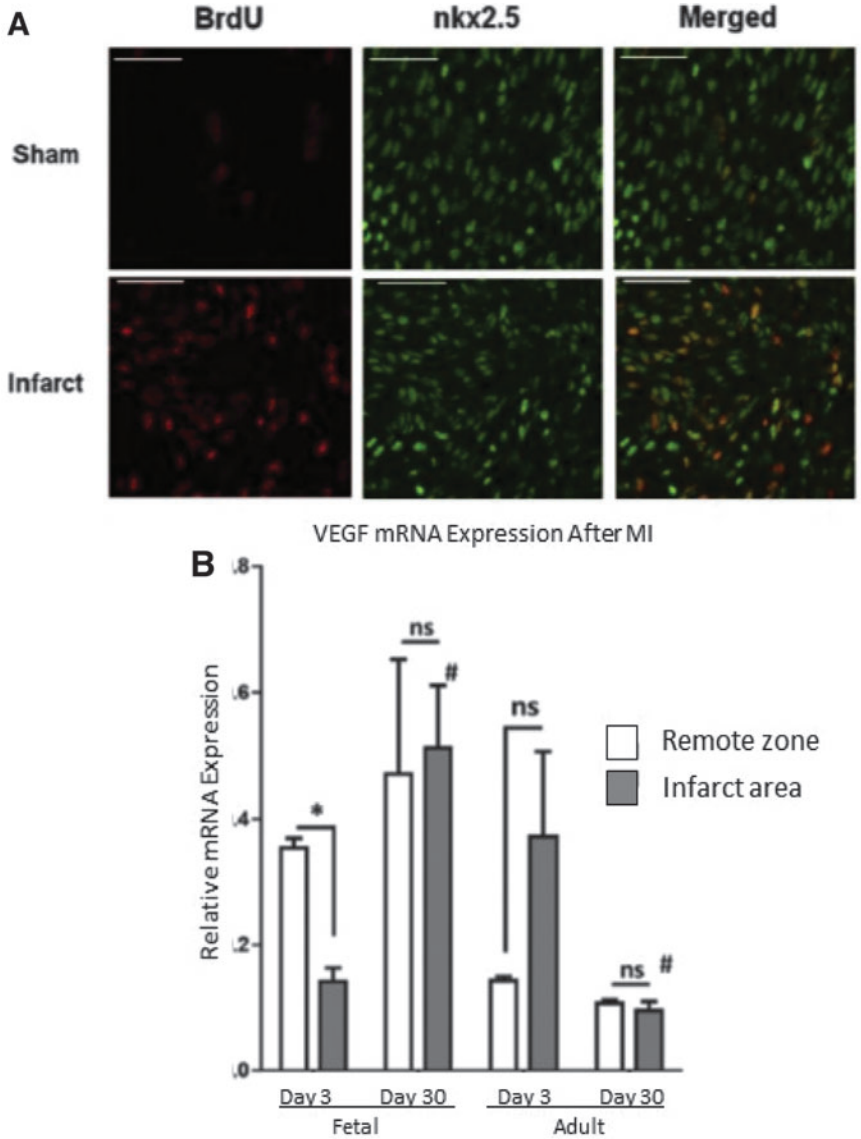

Figure 7. Differential cellular response after MI **(A)** Cardiac cell proliferation contributes to fetal cardiac regeneration following myocardial infarction (MI). Representative immunohistochemistry images for 5-bromo-2-deoxyuridine (BrdU; *red*) and nkx2.5 (*green*) 3 days after MI of the borderzone region of sham and fetal infarcts. **(B)** *VEGF-α* is upregulated in fetal infarcts. Expression of *VEGF-α* in the fetal and adult hearts after MI. Real-time PCR analysis of *VEGF-α* expression in the IA (*shaded bars*) and RZ (*unshaded bars*) of fetal heart (day 3, $n=5$; day 30, $n=5$) and adult heart (day 3, $n=4$; day 30, $n=4$) at 3 and 30 days after myocardial infarction. The *VEGF-α* gene expression was normalized to 18S gene expression. Two-way analysis of variance followed by Fisher's least significant difference *post hoc* test was used to analyze the data. $^{*}p<0.05$ comparing RZ to IA in each group. $^{\#}p<0.0001$ comparing RZ on day 3 to RZ on day 30 or IA on day 3 to IA on day 30. (D = day; mRNA = messenger ribonucleic acid; ns = not significant.) VEGF, vascular endothelial growth factor.

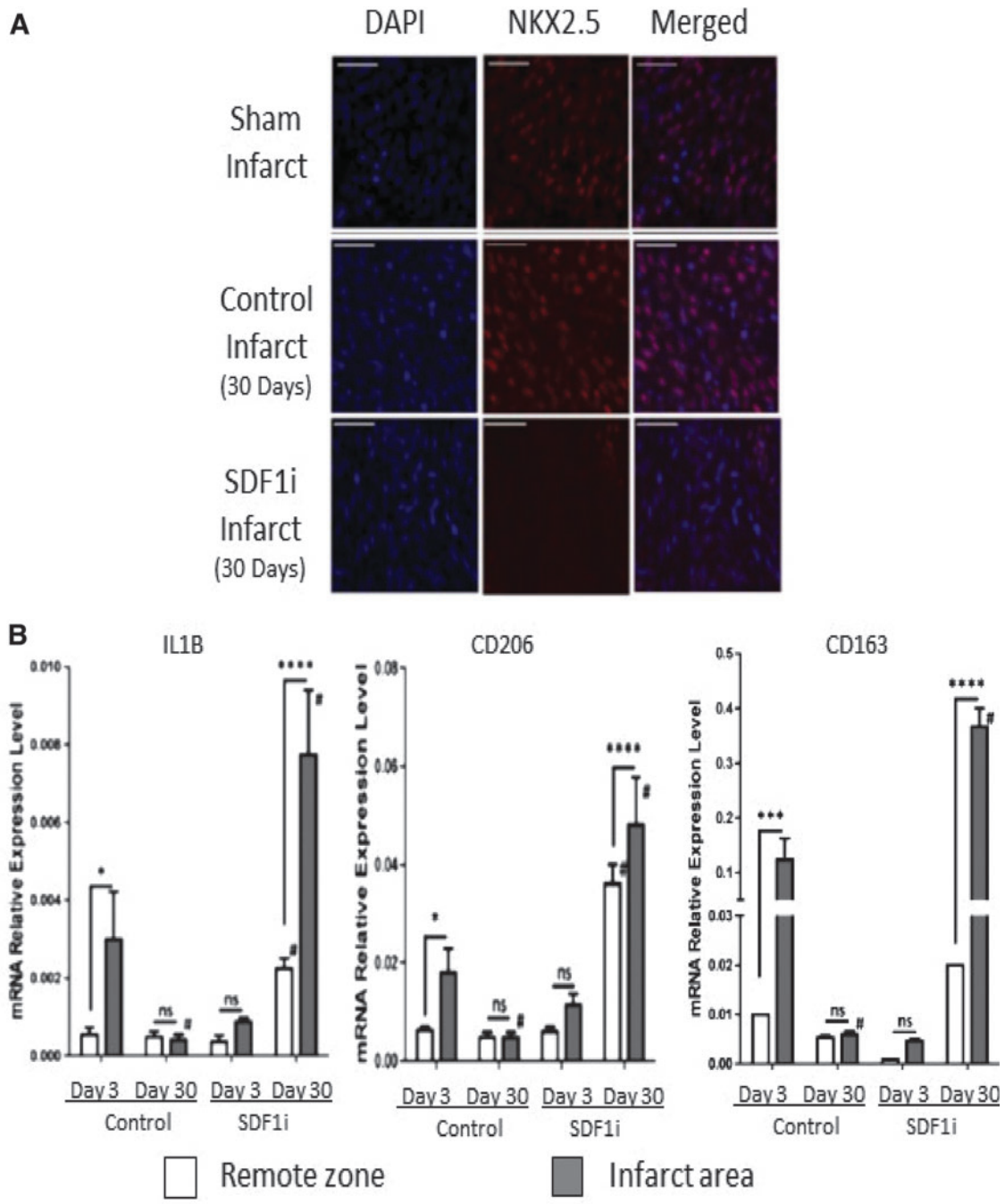

Figure 8. Inhibition of *SDF1α* minimizes regenerative phenotype **(A)** *SDF-1α* inhibition blocks fetal cardiac cell repopulation after myocardial infarction (MI). Representative images show (scale bars = 50 μm) staining with 4′,6-diamidino-2-phenylindole (DAPI; *blue*), immunohistochemistry for nkx2.5 (*red*), and merged DAPI and nkx2.5 of the apex of fetal sham operation and fetal infarct treated with mutant *SDF-1α* transgene (SDFi) at 30 days.**(B)** Real-time PCR analysis of the gene expression of macrophage phenotype markers in the fetal hearts 3 and 30 days after myocardial infarction, with SDF-1α inhibition (day 3, $n=5$; day 30, $n=4$) or without *SDF-1α* inhibition (day 3, $n=5$; day 30, $n=5$). Interleukin-1β (IL-1b), *CD206*, and *CD163* gene expression were calculated after normalizing to 18S. Two-way analysis of variance followed by Fisher's least significant difference *post hoc* test was used to analyze the data. $^{*}p<0.05$, $^{***}p<0.001$, and $^{****}p<0.0001$ comparing RZ (*unshaded bars*) to IA (*shaded bars*) in each group. $\#p<0.0001$ comparing RZ on day 3 to RZ on day 30 or IA on day 3 to IA on day 30. (D = day; mRNA = messenger ribonucleic acid; ns = not significant). SDF-1α, stromal-derived factor-1α.

dition to an impaired regenerative response, fetal infarcts treated with the *SDF1α* mutant manifested macrophage profiles similar to that observed in adult infarcts following MI, with an increased presence of M1, M2a, and M2c macrophages consistent with the prolonged inflammation and ECM remodeling observed in adult infarcts(Fig. 8B).[26]

In vitro evaluation further suggests that baseline differences in the function of adult and fetal cardiac fibroblasts may be responsible for the dif-

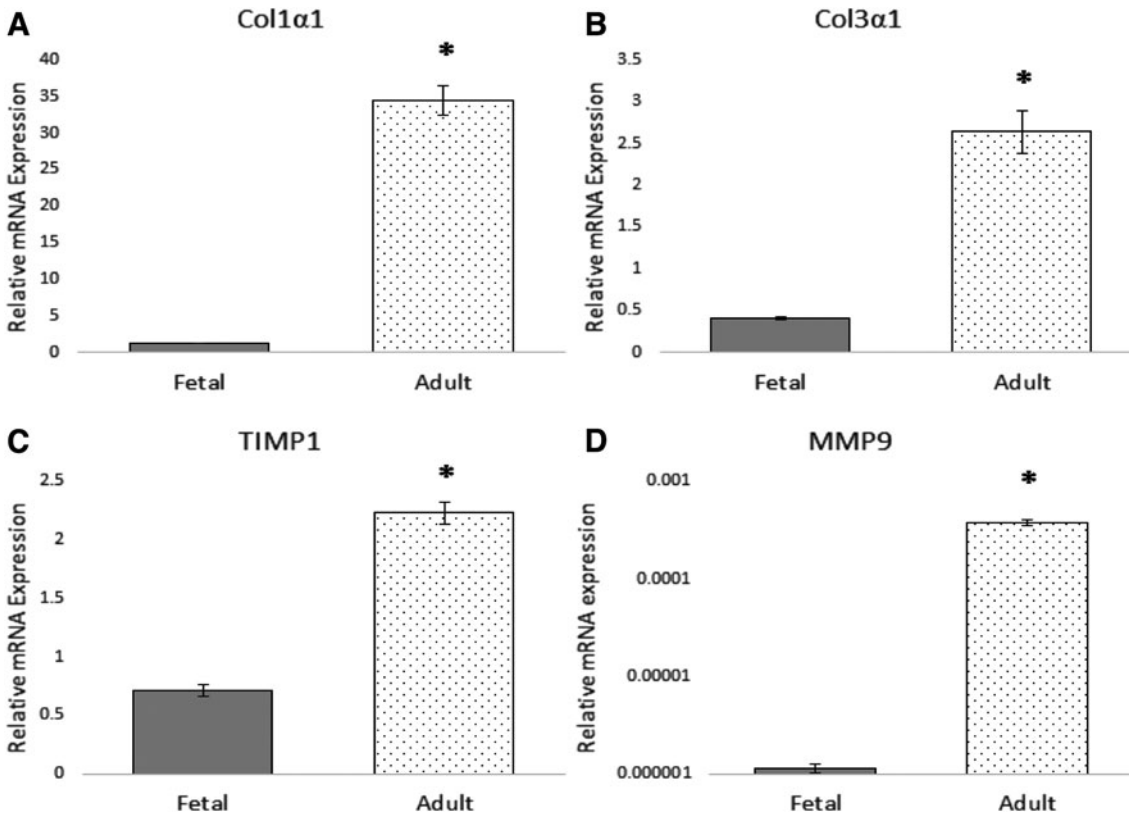

Figure 9. Baseline phenotypic differences in adult and fetal cardiac fibroblasts Adult and fetal cardiac fibroblasts were cultured in DMEM with 10% FBS and 1% antibiotic-antimycotic until 80% confluent. The fibroblasts were then serum starved in DMEM with 1% FBS and 1% antibiotic-antimycotic for 12 h before being harvested for total RNA expression. QPCR demonstrates that adult cardiac fibroblasts have significantly higher expression of *Col1a1* **(A)**, *Col3a1* **(B)**, *TIMP1* **(C)**, and *MMP9* **(D)** than fetal cardiac fibroblasts at baseline. $^*p < 0.05$.

ferential response of ECM regulation observed in our *in vivo* model (Fig. 9). Adult cardiac fibroblasts demonstrate a significant upregulation in the expression of both collagen I (*Col1a1*) and collagen III (*Col3a1*) mRNA at baseline, when compared to fetal cardiac fibroblasts. Similarly, adult cardiac fibroblasts demonstrate marked upregulation of the potent MMP, *MMP-9*, when compared to fetal cardiac fibroblasts. Adult cardiac fibroblasts also demonstrate a significant upregulation of the tissue inhibitor of metalloproteinases 1 (*TIMP1*) compared to fetal cardiac fibroblasts. Treatment of fetal cardiac fibroblasts with *TGFB1* increased the expression of collagen I, collagen III, *MMP-9*, and *TIMP1*.[24]

DISCUSSION

The growing burden of ischemic heart disease necessitates a detailed evaluation of the current models we are using to investigate emerging therapies in the treatment and mitigation of heart failure after MI. This ovine model of myocardial regeneration after MI is the first model to evaluate mechanisms of myocardial regeneration in large mammals, providing insight to the mechanisms by which mammalian hearts can be stimulated to regenerate following an ischemic event. This model has demonstrated key differences in the fetal, regenerative response to MI when compared to the reparative, adult response to MI at every stage of the wound healing response.

During the inflammatory response to MI, the fetal, regenerative model demonstrates decreased infiltration of CD45-positive inflammatory cells compared to the adult response. Global inflammation-related gene expression is also reduced in fetal infarcts 3 and 30 days following MI, compared to the robust upregulation observed in adult infarcts at the same time points. More specifically, fetal infarcts demonstrate only modest upregulation in the expression of proinflammatory cytokines *IL-6* and *IL-8* 3 days following MI, without upregulation observed 30 days following MI, compared to the persistent upregulation of both of these proinflammatory cytokines observed in adult infarcts both 3 and 30 days following MI. Markers of macrophage phenotype are upregulated in both the fetal and adult infarcts 3 days after

MI, but were found to return to baseline by 30 days after MI in fetal infarcts, consistent with the myocardial regeneration observed in fetal hearts. Interestingly, these findings run counter to the results observed in zebrafish and neonatal rodent models of myocardial regeneration, where a marked inflammatory response has been associated with myocardial regeneration.[14] However, these results may differ due to observation of the regenerative response at different time points, as well as use of dramatically different models (a ventricular amputation model vs. a LAD ligation model). Replication of our ovine model of myocardial regeneration using slightly older fetal sheep (105 days gestation) confirmed the decreased inflammatory response we observed in the fetal infarct compared to the adult infarct, although they interestingly noted increased *IL-6* expression in the RZ of fetal hearts, hypothesizing a more mature inflammatory response associated with the more advanced gestational age of the sheep.[29]

During the proliferative phase, the fetal, regenerative response to MI is associated with upregulation of *VEGF* 30 days after MI, whereas *VEGF* is downregulated in adult infarcts 3 and 30 days after MI. The upregulation of *VEGF* seen in the fetal infarct is associated with restoration of vasculature in the fetal infarcts 30 days after MI. In addition to the upregulation of *VEGF* and restoration of vasculature, the fetal, regenerative response to MI is characterized by increased cardiomyocyte proliferation and increased recruitment of CPCs. These findings are supported by studies showing that delivery of *VEGF* to the IA of adult murine hearts reduced infarct size and improved angiogenesis following MI.[30] While Lock *et al.* (2019) look at *BCL-2* as an antiapoptotic protein, *BCL-2* is known to both independently upregulate *VEGF* expression, while also being induced by *VEGF* expression.[29,31] Lock *et al.* (2019) demonstrated that *BCL-2* was upregulated in both adult and fetal infarcts 3 days after MI, while we observed decreased *VEGF* expression in fetal infarcts 3 days after MI, corresponding to the evolving IA and lack of angiogenesis seen histologically at this time point.[26,29] Taken together, these results may suggest that the increased activity of *BCL-2* 3 days postinfarct is predominantly antiapoptotic in nature. Our model contributes significantly to further investigation by enabling evaluation at a later time point (30 days postinfarct), at which time upregulation of *VEGF* gene expression in the fetal infarct is associated with restoration of vasculature within the IA. Further studies are needed to determine if *BCL-2* plays a *VEGF*-independent antiapoptotic role at this time point.

The proliferative and remodeling phases in the fetal, regenerative response to MI are also characterized by decreased fibrosis and scar formation, as well as attenuated upregulation of genes associated with ECM deposition both at 3 and 30 days post-MI, when compared to the response observed in adults hearts. The decreased upregulation of global ECM-related gene expression in fetal infarcts is associated with decreased deposition of collagen, and decreased expression of collagen I and collagen III 30 days post-MI. Most notably, the differential expression of ECM-related genes is associated with a differential expression of the profibrotic growth factor *TGFB1*, with the fetal, regenerative response to MI lacking the TGFB1 upregulation observed in the reparative, fibrotic, adult response to MI.[24] In a mouse model of myocardial reperfusion after MI, *TGFB1* has been seen to peak 6–72 h after reperfusion; however our adult ovine model demonstrated persistent upregulation of *TGFB1* expression 30 days after MI, again demonstrating inconsistencies between rodent models and mammalian models that suggest utility in using a large mammalian experimental model of disease.[32] *TGFB1* is known to be a pleiotropic growth factor, playing a key role in inflammation, recruitment of neutrophils, activation of fibroblasts, and differentiation of macrophages; further studies with this large mammalian model of myocardial regeneration after MI may enable a more thorough understanding of the role that *TGFB1* plays in the development of heart failure following MI.

In vitro evaluation also demonstrates differential regulation of ECM-related genes in adult and fetal cardiac fibroblasts. While adult cardiac fibroblasts also demonstrate a significant upregulation of the *TIMP1* compared to fetal cardiac fibroblasts, the ratio of *MMP9* to *TIMP1* expression is consistent with adult cardiac fibroblasts promoting a more proteolytic milieu than fetal cardiac fibroblasts. These findings suggest that adult cardiac fibroblasts have higher levels of collagen I and collagen III gene expression, as well as a *MMP9:TIMP1* ratio favoring proteolysis, all of which is consistent with the cardiac fibrosis, inflammation, and ventricular wall thinning observed in adult infarcts after MI. Further studies are needed to evaluate the differential response of adult and fetal cardiac fibroblasts to conditions that would mimic the environment of infarcted myocardium

While fibroblasts are considered a hearty and resilient cell population, it is also important to note that variations in cell culture techniques can

significantly affect results of *in vitro* analyses. Notably, some authors have found that plating cardiac fibroblasts on stiff substrates predisposes fibroblasts to activation to the proinflammatory, profibrotic myofibroblast phenotype.[33] Others suggest that the presence of the profibrotic growth factor *TGFB1* in most serum-enriched growth media leads to baseline activation of fibroblasts to a myofibroblast phenotype.[24,32,34] Furthermore, tissue culture methods as basic as selecting an appropriate cell density for plating or passage of cells can promote activation of fibroblasts to a myofibroblast phenotype, with cells plated at a low density being more likely to become activated to the myofibroblast phenotype.[35] Given these findings, we advocate that cells be serum starved in media containing 1% (or less) of FBS 12 h before treatment, and that treatments be performed in media containing 1% (or less) of FBS, to minimize the effect of FBS and myofibroblast activation on the experimental results. We also recommend plating cells at densities >500/mm^2 to minimize the effect that loss of cell-cell interactions may have on myofibroblast activation in the treated cells. By following these basic tenets, we have found that results of our *in vitro* analyses are consistent for experiments performed using cells from passages 2 to 6, with immunohistochemistry demonstrating that only 2.9–5.9% of cardiac fibroblasts become positive for the myofibroblast marker α-smooth muscle actin (αSMA) when cultured under these conditions (unpublished data).

We believe that our ovine large mammalian model of myocardial regeneration after MI is a more physiologically representative model with which to study the myocardial response to ischemia, as well as the physiology underlying the fetal regenerative response. However, no model is perfect. Compared to rodents, sheep have longer gestations, are less fecund, and are more expensive to house and tend to. Adult sheep also possess less mononucleate cardiomyocytes in adulthood than humans; however, this physiologic difference makes sheep less likely to regenerate functional myocardium, making it a more conservative model than using zebrafish or rat models.[15] Rodent models of myocardial regeneration following MI are often used because of the ease of manipulating mechanistic pathways using lentiviral transfection; this mechanistic manipulation is also feasible in our ovine model of myocardial regeneration following MI, as described above. Furthermore, technologies such as CRISPR/Cas-9 make the development of large animal transgenic models more feasible, broadening the applicability of large animal models in translational research.[36,37]

INNOVATION

The foundation of cardiac regeneration research was built upon use of zebrafish and rodent models. However, animal models more representative of human physiology may improve the identification of therapeutic target pathways and be more representative models to test therapies derived from canonical zebrafish and rodent experiments. Worldwide, over 20% of all deaths are attributable to the effects of ischemic heart disease.[38] Use of this large mammalian model of myocardial regeneration after MI may expedite identification of therapies key to mitigating the growing burden of disease attributable to ischemic heart disease and heart failure.

ACKNOWLEDGMENTS AND FUNDING SOURCES

The authors would like to thank the members of the Laboratory for Fetal and Regenerative Biology for their support: Junyi Hu, Junwang Xu, Kerri York, Lindel Dewberry, and Sarah Hilton. Dr. Ken Liechty is supported by NIH grants 5R01DK105010 and 1R01DK118793.

AUTHOR DISCLOSURE AND GHOSTWRITING

No competing financial interests exist. The content of this article was expressly written by the author(s) listed. No ghostwriters were used to write this article. All writing was performed by M.M.H. and C.Z., and all experiments were performed or overseen by M.M.H., C.Z., or K.W.L.

ABOUT THE AUTHORS

Maggie M. Hodges, MD, MPH, is a General Surgery resident at the University of Colorado, performing research focused upon understanding fetal mammalian myocardial regeneration. Dr. Hodges is a resident member of the American College of Surgeons, the Wound Healing Society, and the Association for Academic Surgery. **Carlos Zgheib, PhD,** is an Assistant Professor in the Department of Surgery at the University of Colorado, whose research focuses upon tissue regeneration. Dr. Zgheib is a member of the Wound Healing Society, the American Association for the Advancement of Science, the American Heart Association, and the Honor Society of Phi Kappa Phi for Superior Scholarship and Academic Excellence.

Kenneth W. Liechty, MD, is the Sandy Wolf Chair in Maternal Fetal Surgery, Director of Pediatric Surgery Basic and Translational Research, and co-Director of the Colorado Fetal Care Center at Children's Hospital Colorado on the University of Colorado Anschutz Medical Campus. He is a fellow of the American College of Surgeons and the American Academy of Pediatrics, and a member of the American Pediatric Surgical Association, the Wound Healing Society, and the Association for Academic Surgery. Dr. Liechty is NIH funded and nationally recognized for his expertise in wound healing research.

KEY FINDINGS

- Compared to a reparative, adult response, the fetal mammalian response to MI is associated with the following:
  - Decreased inflammation both 3 and 30 days after MI
  - Decreased ECM production and ECM-related gene expression
  - Increased VEGF expression and absence of TGFB1 upregulation
  - Increased angiogenesis
  - Regeneration of fully functional myocardium within 30 days after MI
- Ideal animal models in experimental research should reproduce human physiology and function as closely as possible. Large mammalian models of myocardial regeneration after MI, including the ovine model described herein, may provide improved translation of research findings to clinical practice.

REFERENCES

1. Yusuf S, Reddy S, Ounpuu S, Anand S. Global burden of cardiovascular diseases: part I: general considerations, the epidemiologic transition, risk factors, and impact of urbanization. Circulation 2001;104:2746–2753.
2. Blair JEA, Huffman M, Shah SJ. Heart failure in North America. Curr Cardiol Rev 2013;9:128–146.
3. Moran AE, Forouzanfar MH, Roth GA, Mensah GA, Ezzati M, Flaxman A, et al. The global burden of ischemic heart disease in 1990 and 2010: the Global Burden of Disease 2010 study. Circulation 2014;129:1493–1501.
4. Mozaffarian D, Benjamin EJ, Go AS, Arnett DK, Blaha MJ, Cushman M, et al. Heart disease and stroke statistics—2015 update: a report from the American Heart Association. Circulation 2015;131:e29–e322.
5. Gerber Y, Weston SA, Enriquez-Sarano M, Berardi C, Chamberlain AM, Manemann SM, et al. Mortality associated with heart failure after myocardial infarction: a contemporary community perspective. Circ Heart Fail 2016;9:e002460.
6. Li A-H, Liu PP, Villarreal FJ, Garcia RA. Dynamic changes in myocardial matrix and relevance to disease: translational perspectives. Circ Res 2014;114:916–927.
7. Travers JG, Kamal FA, Robbins J, Yutzey KE, Blaxall BC. Cardiac fibrosis: the fibroblast awakens. Circ Res 2016;118:1021–1040.
8. Dobaczewski M, Gonzalez-Quesada C, Frangogiannis NG. The extracellular matrix as a modulator of the inflammatory and reparative response following myocardial infarction. J Mol Cell Cardiol 2010;48:504–511.
9. Dobaczewski M, de Haan JJ, Frangogiannis NG. The extracellular matrix modulates fibroblast phenotype and function in the infarcted myocardium. J Cardiovasc Transl Res 2012;5:837–847.
10. Poss KD, Wilson LG, Keating MT. Heart regeneration in zebrafish. Science 2002;298:2188–2190.
11. Jopling C, Sleep E, Raya M, Martí M, Raya A, Izpisúa Belmonte JC. Zebrafish heart regeneration occurs by cardiomyocyte dedifferentiation and proliferation. Nature 2010;464:606–609.
12. Smart N, Dubé KN, Riley PR. Epicardial progenitor cells in cardiac regeneration and neovascularisation. Vascul Pharmacol 2013;58:164–173.
13. Milani-Nejad N, Janssen PML. Small and large animal models in cardiac contraction research: advantages and disadvantages. Pharmacol Ther 2014;141:235–249.
14. Porrello ER, Mahmoud AI, Simpson E, Hill JA, Richardson JA, Olson EN, et al. Transient regenerative potential of the neonatal mouse heart. Science 2011;331:1078–1080.
15. Botting KJ, Wang KCW, Padhee M, McMillen IC, Summers-Pearce B, Rattanatray L, et al. Early origins of heart disease: low birth weight and determinants of cardiomyocyte endowment. Clin Exp Pharmacol Physiol 2012;39:814–823.
16. Reiser PJ, Portman MA, Ning XH, Schomisch Moravec C. Human cardiac myosin heavy chain isoforms in fetal and failing adult atria and ventricles. Am J Physiol Heart Circ Physiol 2001;280:H1814–H1820.
17. Puente XS, Sánchez LM, Overall CM, López-Otín C. Human and mouse proteases: a comparative genomic approach. Nat Rev Genet 2003;4:544–558.
18. Herdrich BJ, Danzer E, Davey MG, Allukian M, Englefield V, Gorman JH, et al. Regenerative healing following foetal myocardial infarction. Eur J Cardio-Thorac Surg 2010;38:691–698.
19. Lang RM, Badano LP, Mor-Avi V, Afilalo J, Armstrong A, Ernande L, et al. Recommendations for cardiac chamber quantification by echocardiography in adults: an update from the american society of echocardiography and the european association of, cardiovascular imaging. Eur Heart J Cardiovasc Imaging 2016;17:412.
20. Chrominski K, Tkacz M. Comparison of high-level microarray analysis methods in the context of result consistency. PLoS One 2015;10:e0128845.
21. Graham NS, May ST, Daniel ZCTR, Emmerson ZF, Brameld JM, Parr T. Use of the Affymetrix Human GeneChip array and genomic DNA hybridisation probe selection to study ovine transcriptomes. Animal 2011;5:861–866.
22. Schmittgen TD, Livak KJ. Analyzing real-time PCR data by the comparative C(T) method. Nat Protoc 2008;3:1101–1108.
23. Zgheib C, Allukian MW, Xu J, Morris MW, Caskey RC, Herdrich BJ, et al. Mammalian fetal cardiac regeneration after myocardial infarction is associated with differential gene expression compared with the adult. Ann Thorac Surg 2014;97:1643–1650.
24. Hodges MM, Zgheib C, Xu J, Hu J, Dewberry LC, Hilton SA, et al. Differential expression of transforming growth factor-B1 is associated with fetal regeneration after myocardial infarction. Ann Thorac Surg 2019;108:59–66.
25. Soonpaa MH, Field LJ. Survey of studies examining mammalian cardiomyocyte DNA synthesis. Circ Res 1998;83:15–26.
26. Zgheib C, Hodges MM, Allukian MW, Xu J, Spiller KL, Gorman JH, et al. Cardiac progenitor cell recruitment drives fetal cardiac regeneration by

enhanced angiogenesis. Ann Thorac Surg 2017; 104:1968–1975.

27. Allukian M, Xu J, Morris M, Caskey R, Dorsett-Martin W, Plappert T, et al. Mammalian cardiac regeneration after fetal myocardial infarction requires cardiac progenitor cell recruitment. Ann Thorac Surg 2013;96:163–170.

28. Morris MW, Liechty KW. Cardiac progenitor cells in myocardial infarction wound healing: a critical review. Adv Wound Care 2013;2:317–326.

29. Lock MC, Darby JRT, Soo JY, Brooks DA, Perumal SR, Selvanayagam JB, et al. Differential response to injury in fetal and adolescent sheep hearts in the immediate post-myocardial infarction period. Front Physiol 2019;10:208.

30. Zangi L, Lui KO, von Gise A, Ma Q, Ebina W, Ptaszek LM, et al. Modified mRNA directs the fate of heart progenitor cells and induces vascular regeneration after myocardial infarction. Nat Biotechnol 2013;31:898–907.

31. Iervolino A, Trisciuoglio D, Ribatti D, Candiloro A, Biroccio A, Zupi G, Del Bufalo D. BCL-2 overexpression in human melanoma cells increases angiogenesis through VEGF mRNA stabilization and HIF-1 mediated transcriptional activity. FASEB J 2002;16:1453–1455.

32. Hanna A. Frangogiannis NG. The role of the TGF-B superfamily in myocardial infarction. Front Cardiovasc Med 2019;6:140.

33. Wang J, Chen H, Seth A, McCulloch CA. Mechanical force regulation of myofibroblast differentiation in cardiac fibroblasts. Am J Physiol Heart Circ Physiol 2003;285:H1871–H1881.

34. Khouw IM, van Wachem PB, Plantinga JA, Vujaskovic Z, Wissink MJ, de Leij LF, et al. TGF-beta and bFGF affect the differentiation of proliferating porcine fibroblasts into myofibroblasts in vitro. Biomaterials 1999;20:1815–1822.

35. Masur SK, Dewal HS, Dinh TT, Erenburg I, Petridou S. Myofibroblasts differentiate from fibroblasts when plated at low density. Proc Natl Acad Sci U S A 1996;93:4219–4223.

36. Fan Z, Perisse IV, Cotton CU, Regouski M, Meng Q, Domb C, et al. A sheep model of cystic fibrosis generated by CRISPR/Cas9 disruption of the CFTR gene. JCI Insight 2018;3:e123529.

37. Vilarino M, Rashid ST, Suchy FP, McNabb BR, van der Meulen T, Fine EJ, et al. CRISPR/Cas9 microinjection in oocytes disables pancreas development in sheep. Sci Rep 2017;7:17472.

38. Institute for Health Metrics and Evaluation (IHME). GBD Compare [Internet]. Seattle, WA: University of Washington; 2015 [cited 2018 Oct 15]. http://vizhub.healthdata.org/gbd-compare (last accessed October 15, 2018).

39. Pylatiuk C, Sanchez D, Mikut R, Alshut R, Reischl M, Hirth S, et al. Automatic zebrafish heartbeat detection and analysis for zebrafish embryos. Zebrafish 2014;11:379–383.

40. Hu N, Yost HJ, Clark EB. Cardiac morphology and blood pressure in the adult zebrafish. Anat Rec 2001;264:1–12.

41. Shih Y-H, Zhang Y, Ding Y, Ross CA, Li H, Olson TM, et al. Cardiac transcriptome and dilated cardiomyopathy genes in zebrafish. Circ Cardiovasc Genet 2015;8:261–269.

42. Wills AA, Holdway JE, Major RJ, Poss KD. Regulated addition of new myocardial and epicardial cells fosters homeostatic cardiac growth and maintenance in adult zebrafish. Dev Camb Engl 2008;135:183–192.

43. Paradis AN, Gay MS, Zhang L. Binucleation of cardiomyocytes: the transition from a proliferative to a terminally differentiated state. Drug Discov Today 2014;19:602–609.

Abbreviations and Acronyms

BCL-2 = B-cell lymphoma 2
BZ = border zone
CPC = cardiac progenitor cell
ECM = extracellular matrix
EF = ejection fraction
FBS = fetal bovine serum
IA = infarct area
IM = intramuscular
IV = intravenous
LAD = left anterior descending artery
LR = Lactated Ringer's
LV EDV = left ventricular end-diastolic volume
LVEF = left ventricular ejection fraction
LV ESV = left ventricular end-systolic volume
MI = myocardial infarctions
MMP = matrix metalloproteinase
MHC = myosin heavy chain
PBS = phosphate-buffered saline
PCR = polymerase chain reaction
ROS = reactive oxygen species
RZ = remote zone
SDF1α = stromal-derived factor 1α
TGFB-1 = transforming growth factor beta-1
TIMP = tissue inhibitor of metalloproteinase
VEGF = vascular endothelial growth factor